

Research Article

Study on the Mitigative Effect of Controlled Permeable Formwork (CPF) Liner on Early-Age Shrinkage of Box-Girder Concrete

Jianxiong Ye,¹ Linwen Yu ,^{1,2} and Yong Chen¹

¹College of Materials Science and Engineering, Chongqing University, 400045 Chongqing, China

²The State Key Laboratory of Green Building Materials, 100024 Beijing, China

Correspondence should be addressed to Linwen Yu; linwen.yu@cqu.edu.cn

Received 16 April 2019; Accepted 9 August 2019; Published 10 September 2019

Academic Editor: Luigi Nicolais

Copyright © 2019 Jianxiong Ye et al. This is an open access article distributed under the Creative Commons Attribution License, which permits unrestricted use, distribution, and reproduction in any medium, provided the original work is properly cited.

Because of its high binder content and severe construction environment, early-age cracking is one of the most important threats to concrete used in continuous box-girder bridge structures. In this study, controlled permeable formwork (CPF) liner was used to mitigate the early-age shrinkage and reduce the early-age cracking risk of box-girder concrete. Early-age shrinkage was measured by a noncontact method and started at 30 min after adding mix water until 7 d. Internal relative moisture content and pore distribution tests were also carried out to reveal the working mechanism of CPF liner. The results show that covering the concrete surface with CPF liner decreased early-age shrinkage significantly. Under the temperature of 20°C and the relative humidity of 60%, two-surface-covering and three-surface-covering CPF liner on concrete decreased the shrinkage by 44% and 48%, respectively, at 7 d compared with concrete without CPF liner covered on it. The main reason is that CPF liner enhanced the internal relative moisture content and resulted in better performance of the surface concrete.

1. Introduction

Continuous box-girder bridge structural systems have been widely used and developed rapidly all over the world. Normally, the concrete used in continuous box-girder bridge structures needs a high slump value due to complex construction methods and its high compressive strength. Furthermore, most of the continuous box-girder bridges service in valleys and gorges where they are quite windy. Because of the high binder content of box-girder concrete and severe service environment, early-age cracking of concrete is an important risk which threatens the safety and durability of continuous box-girder bridge structures.

Numerous techniques have been proposed to mitigate early-age shrinkage and cracking, such as optimizing concrete mix proportion [1], blending shrinkage-reducing agent or expansive agent [2, 3], applying internal curing with super absorbent polymer (SAP) or light-weight aggregate [4, 5], and moist curing [6]. Moist curing is one of the most effective methods to inhibit early-age shrinkage and cracking; however, it is not always suitable to cure the box-girder

concrete. Moist curing is normally applied in the form of water spraying, ponding, or damp covering. It is difficult to cover the outer surface of the bottom plate damply, and the frequent wind in the service environment makes water spraying not feasible.

Controlled permeable formwork (CPF) liner is an effective technology that reduces the sensitivity of the concrete to poor site curing and improves the quality of cover concrete [7]. A lot of studies have been carried out to investigate the improvement of appearance, surface hardness, mechanical performance, and durability properties of concrete caused by the utilization of CPF liner. The improvement of surface appearance has been confirmed [7–14]. The surface of concrete cast with CPF liner had a smooth and darker surface without any visible defects. Figueiras et al. [7], Law et al. [8, 14], Kothandaraman and Kandasamy [10, 11], and Liu et al. [15] found that surface hardness, water absorption by capillarity, wear resistance, and abrasion resistance of concrete casted with CPF liner was significantly higher than the same concrete cast traditionally. Adam et al. [13] and Law et al. [14] revealed that CPF liner increased the

surface properties of concrete significantly, while the improvement on bulk properties of the concrete, including resistivity, ultrasonic pulse velocity (UPV), and surface hardness, was limited. Kothandaraman et al. [12] confirmed that CPF liner had the same efficiency on self-compacting concrete. Adam et al. [13] and Law et al. [14] reported that not only ordinary Portland cement concrete but also concrete blending fly ash and blast furnace slag could be improved by CPF liner.

Contrast with lots of research focused on the effect of CPF liner on the quality and durability of cover concrete, almost no attention has been paid on its effect on early-age shrinkage and cracking resistance of concrete. In order to discuss the feasibility of using CPF liner to inhibit early-age cracking risk of box-girder concrete, this paper investigates early-age shrinkage of concrete cast with CPF liner under different environment conditions. Internal relative moisture content and pore distribution are also tested to reveal the working mechanism of CPF liner.

2. Materials and Methods

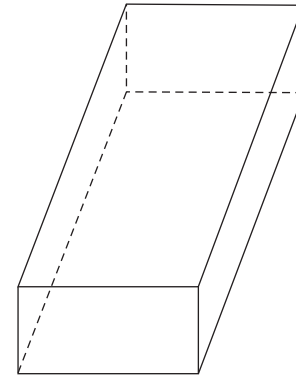
2.1. Materials. Concrete was produced using P.O 42.5 cement conforming to the Chinese standard GB 175-2007. Its specific surface area was $340 \text{ m}^2/\text{kg}$, specific gravity was 3.04 g/cm^3 , initial and final setting time was 138 min and 220 min, respectively, and compressive strength at 3 d and 28 d was 25.3 MPa and 46.0 MPa, respectively. River sand with a specific gravity of 2.68 g/cm^3 and fineness modulus of 3.0 was used, and the percentage of particles smaller than $80 \mu\text{m}$ was 1.9%. Crushed limestone aggregate with a maximum size of 20 mm and a specific gravity of 2.72 g/cm^3 was used. Tap water was used to mix the concrete. Polycarboxylate superplasticizer was used to achieve a desired slump. The unit weight of CPF liner was 380 g/cm^2 , and the thickness was 1.04 mm. The mix proportions of concrete are presented in Table 1. The slump was 215 mm, and the slump flow was 500 mm. The compressive strength of concrete at 3 d and 28 d was 44.8 MPa and 72.4 MPa, respectively.

2.2. Experiment Design. Three series of specimens were tested in this paper. In Series 1, concrete was cast in impermeable moulds (steel mould). In Series 2, two lateral surfaces of the moulds were covered with CPF liner. In Series 3, CPF liner was used to cover the bottom surface and two lateral surfaces of the moulds. Figure 1 demonstrates the paste method of CPF liner.

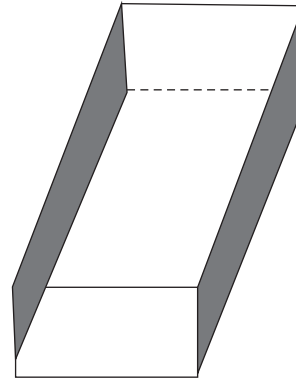
2.3. Early-Age Shrinkage Test. Early-age shrinkage was measured using a noncontact method. Concrete was poured into moulds with a dimension of $100 \text{ mm} \times 100 \text{ mm} \times 515 \text{ mm}$. To limit friction and seal joints, the inner walls of specimen moulds were coated with Teflon tapes and mould surfaces were covered with two layers of plastic sheet. A plastic probe was placed in the end of the specimen, and then, a noncontact laser transducer was used to record the linear movement of the plastic probe. The experimental set-up is illustrated in Figure 2

TABLE 1: Mix proportions of concrete (kg/m^3).

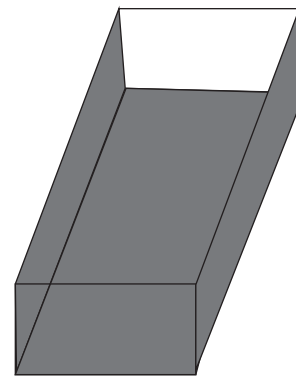
Cement	Fly ash	Slag	Sand	Coarse aggregate	Water	Superplasticizer
385	50	70	790	1005	150	10



(a)



(b)



(c)

FIGURE 1: Schematic of CPF liner paste method. (a) No CPF. (b) Lateral surfaces covered by CPF. (c) Three surfaces covered by CPF.

[16]. Moulds were filled with concrete in two layers and compacted on a vibrating table until no air appeared at the surface. Immediately after casting, specimens were subjected to four different environment conditions ($20 \pm 2^\circ\text{C}/60 \pm 5\% \text{ RH}$, $20 \pm 2^\circ\text{C}/80 \pm 5\% \text{ RH}$, $30 \pm 2^\circ\text{C}/60 \pm 5\% \text{ RH}$, $30 \pm 2^\circ\text{C}/80 \pm 5\% \text{ RH}$). Plastic shrinkage measurements were started at 30 min

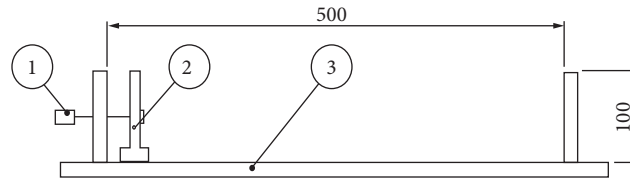


FIGURE 2: Illustration of the test set-up for early-age shrinkage (all dimensions in mm). Notes: 1 represents the part connecting with the laser sensor. 2 represents the part embedded in concrete. 3 represents the mould.

after adding mix water and recorded automatically every 10 min on a computer until 7 d.

2.4. Internal Relative Moisture Content Test. The internal relative moisture content of concrete was measured by a method using electrodes proposed by Ichise et al. [17]. Electrical resistance was measured by embedding a miniature electrode array in the specimens. The probe comprised six electrode pairs mounted on a small Plexiglas former, and each electrode consisted of a stainless steel pin (1.5 mm diameter) which was sleeved to expose a 2 mm tip; in each electrode pair, the pins had a centre-to-centre spacing of 5 mm. The pairs of electrodes were positioned at 5, 10, 20, 30, 40, and 50 mm from the exposed surface. The resistance between pairs of electrodes was measured by an LCR meter, with an impressed voltage of AC 1 V, and a frequency of 1 kHz was selected [18]. The calibration tests to estimate the relative moisture content by electrical resistance were carried out according to the method described in [19].

Specimens with a dimension of 150 mm × 150 mm × 200 mm were casted. When CPF liner was used, the electrical probes were mounted on the surface covered by CPF liner (Figure 3).

2.5. Mercury Intrusion Porosimetry (MIP). For MIP tests, the concrete was cast in cubic moulds with a side length of 100 mm. The specimens were exposed at $30 \pm 2^\circ\text{C}$ and $60 \pm 5\%$ RH for 3 days. A small sample with a volume of around $8 \times 8 \times 8 \text{ mm}^3$ was collected from the lateral surface of each cubic specimen. Subsequently, the small samples for MIP tests were immersed in ethyl alcohol for 24 h to avoid any possible hydration. Afterwards, the samples were dried at 45°C in a vacuum oven until a constant mass was obtained. The MIP test was conducted on a Micromeritics Autopore Mercury Porosimeter IV 9500 with 50000 Psi pressure.

3. Results and Discussion

3.1. Early-Age Shrinkage. The early-age shrinkage of three series of specimens, no CPF liner, two lateral surfaces with CPF liner, and three surfaces (including two lateral surfaces and the bottom surface) with CPF liner, was measured under different environment conditions. Figures 4(a)–4(d) show the shrinkage development of concrete samples under different temperature and relative humidity. In the legend, NTY presents concrete without CPF liner, BMY and TMY means two-surface-covering and three-surface-covering concrete, respectively, with CPF liner separately.

Plastic shrinkage of all specimens shows a similar developing trend regardless of the environment condition and the covering method of CPF liner. In the first hours, plastic shrinkage increased drastically followed by a short steady period, and then, it climbed gently until the end of the testing duration. The development of plastic shrinkage could be divided into three phases, the sharp-grow phase (Phase I), the slight fluctuation phase (Phase II), and the gentle-increase phase (Phase III). The Phase I duration of samples covered by CPF liner was quite different from that of concrete without CPF liner. When there was no CPF liner covered on the surfaces, the dramatic growth phase (Phase I) lasts for around 10 to 12 hours, while the Phase I duration of samples covered with CPF liner was only about 5 to 7 hours. For the same environment condition, the shrinkage rate in the first phase was almost the same for all the samples without CPF liner and with two or three surfaces covered by CPF liner. The environment temperature and relative humidity had significant impact on the shrinkage rate in the first phase. Comparing the four figures, it could be noted that the shrinkage rate in Phase I increased with the increase of temperature and decreased with the increase of relative humidity because higher temperature and lower relative humidity resulted in a higher water evaporation rate. Shrinkage in the first phase was mainly caused by bleeding and settlement of plastic shrinkage [20, 21]. The increased shrinkage rate of samples with and without CPF liner was identical under certain environment conditions because the samples under the same temperature, relative humidity, and wind speed had the same water evaporation rate.

Some volume swelling was found in the slight fluctuation phase (Phase II). This phenomenon was also noticed in previous research [20, 22, 23]. Zhang et al. [23] reported a maximum swelling strain of $70 \mu\text{m}/\text{m}$ and $250 \mu\text{m}/\text{m}$ for C30 and C80 concrete, respectively. Kucharczyková et al. [20] found that the swelling phenomenon in the early age was strongly dependent on the cement content and water-to-cement ratio of concrete. They attributed the swelling phenomenon partially to thermal expansion induced by the hydration heat and principally to the reabsorption of free water after the transformation of concrete from a plastic to a solid state. During the compaction period, water tends to migrate to the surface of concrete. In the present investigation, much water in the fresh concrete was absorbed by the CPF liner. So, the swelling degree of concrete covered with CPF liner was higher than that with no CPF liner. The reabsorption of water stored in the CPF liner was the most important reason.

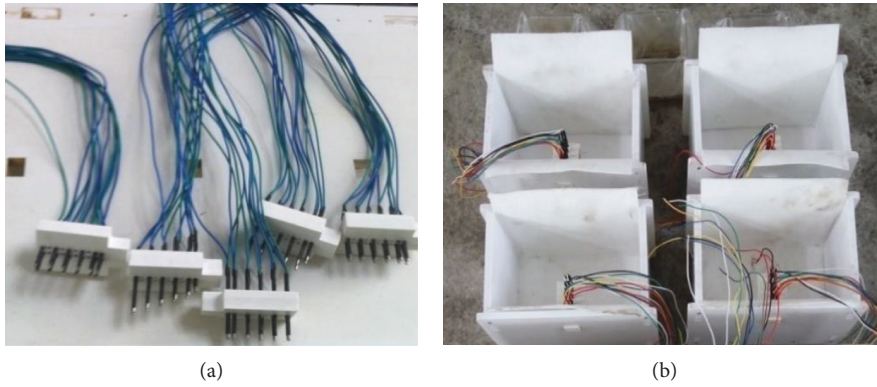


FIGURE 3: Electrical probes and their installation.

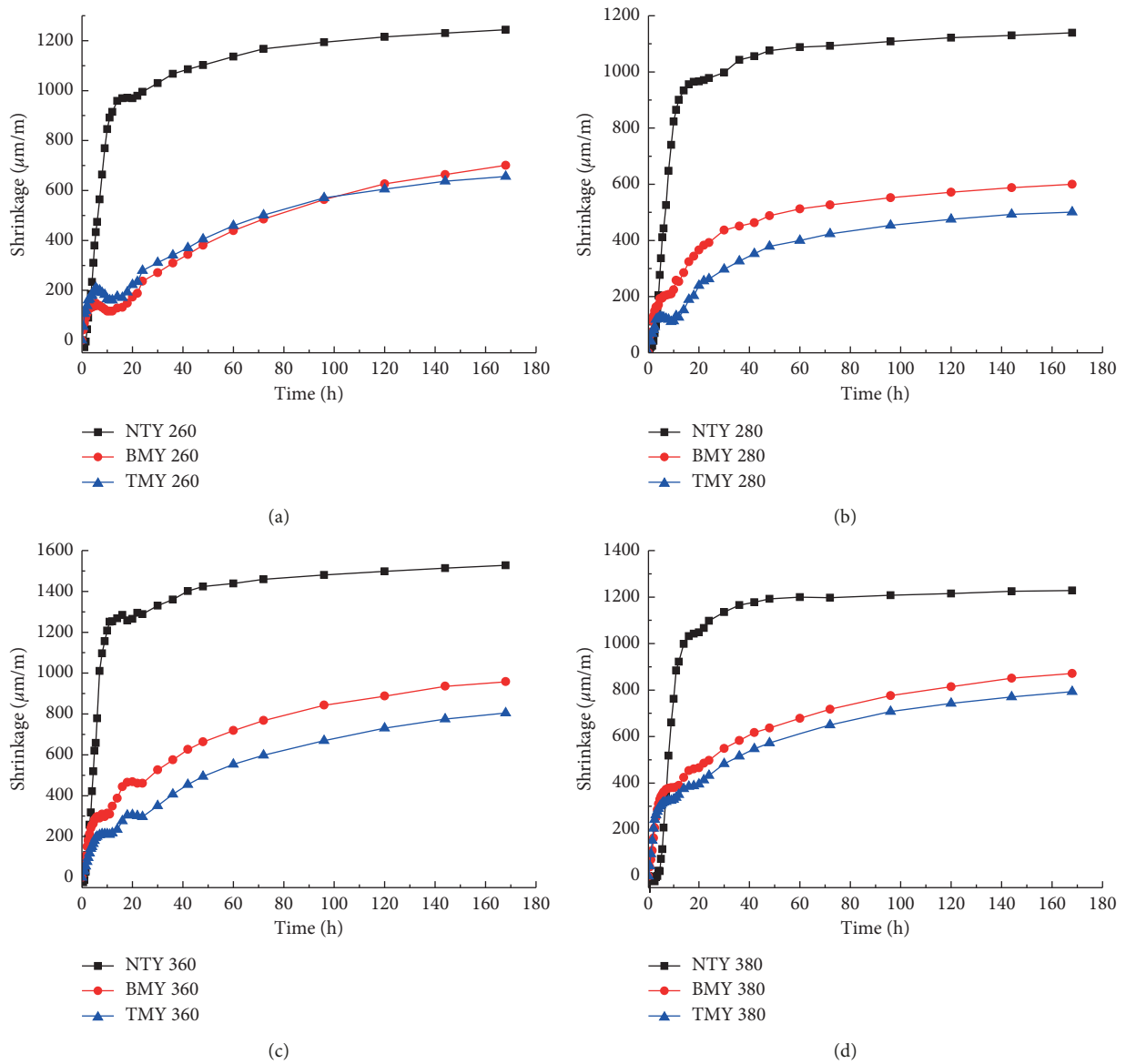


FIGURE 4: Early-age shrinkage of concrete under different environment conditions. (a) $20 \pm 2^\circ\text{C}$, $60 \pm 5\%$ RH. (b) $20 \pm 2^\circ\text{C}$, $80 \pm 5\%$ RH. (c) $30 \pm 2^\circ\text{C}$, $60 \pm 5\%$ RH. (d) $30 \pm 2^\circ\text{C}$, $80 \pm 5\%$ RH.

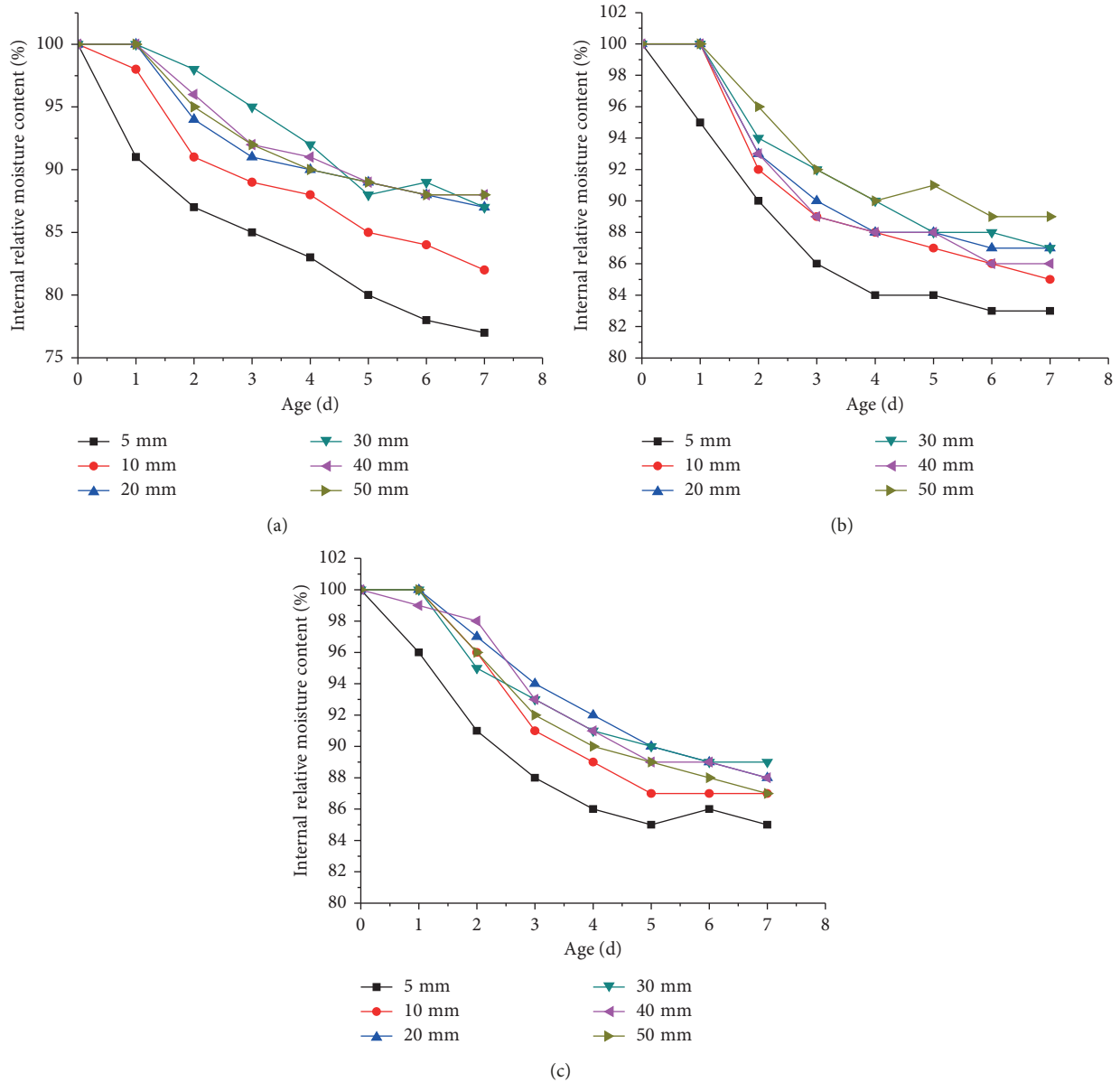


FIGURE 5: Internal relative moisture content of concrete under 20°C, 60% RH. (a) No CPF liner. (b) Lateral surfaces covered by CPF liner. (c) Three surfaces covered by CPF liner.

In the third phase, the increasing rate of shrinkage declined markedly. Contrasting with the total shrinkage, the strain rate of the samples covered with CPF liner was obviously higher than that without CPF liner cover, and the rate of shrinkage of the latter was greater. From Figure 4, it is obvious that the total shrinkage at 7 d of the specimen without CPF liner is much higher than those with CPF liner. The early-age shrinkage increased with the increase of temperature and decrease of relative humidity because the water evaporation rate was increased.

Increasing temperature or decreasing relative humidity of the environment results in the increase of early-age shrinkage because water evaporation becomes more serious. Covering CPF liner on the concrete surface could decrease early-age shrinkage effectively, and three-surface-covering

performed better than two-surface-covering. Under the temperature of 20°C and the relative humidity of 60%, two-surface-covering and three-surface-covering CPF liner decreased the shrinkage at 7 d by 44% and 48%, respectively.

3.2. Internal Relative Moisture Content. The internal relative moisture content of concrete was recorded once a day, and the results are presented in Figures 5 and 6.

It could be found in the figures that the internal relative moisture content decreased with the prolongation of concrete age, and the relative moisture content close to the surface was remarkably lower. Figures 5(a) and 6(a) show the variation of internal relative moisture content of samples without CPF liner. The relative moisture content at the depth

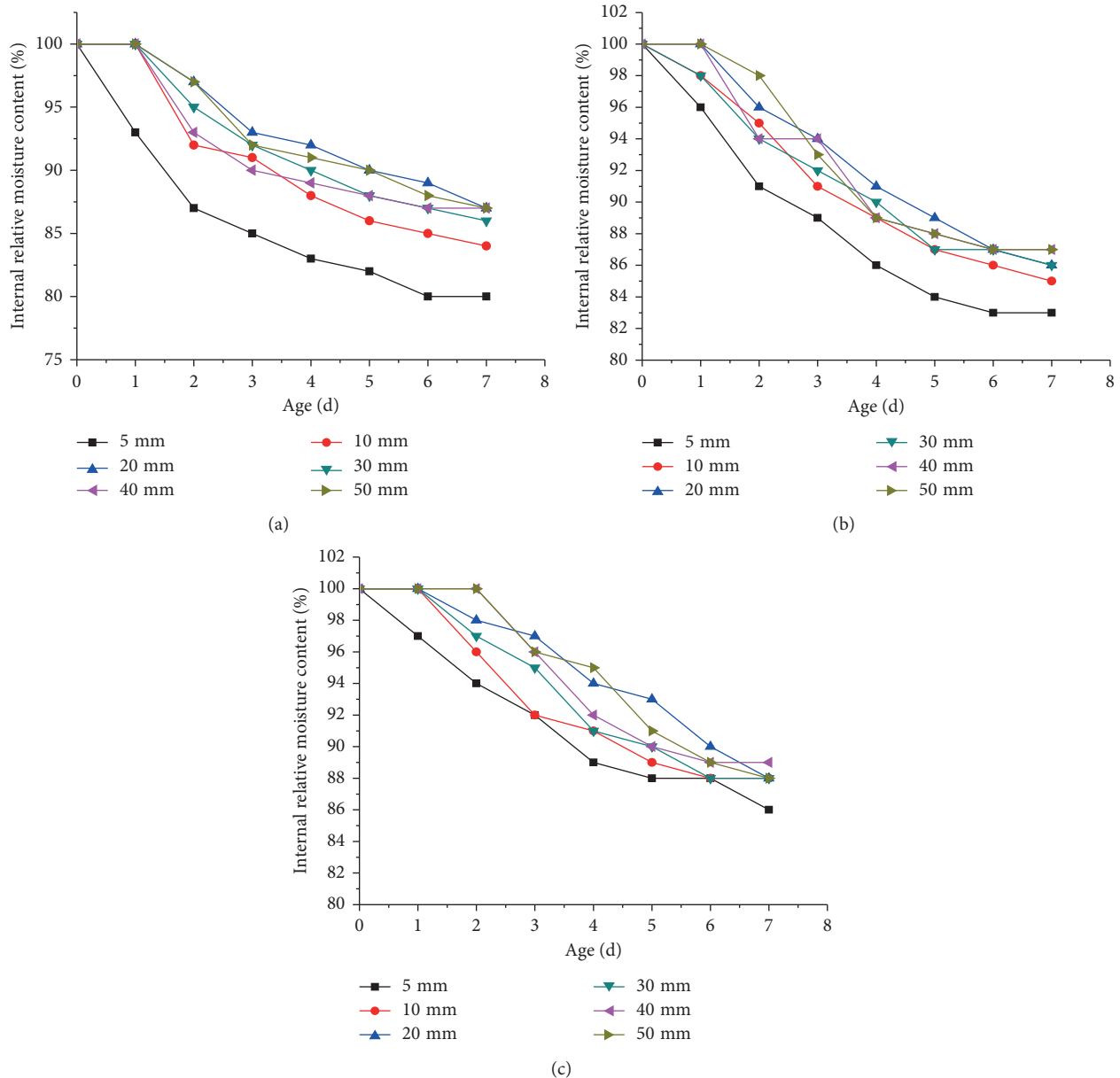


FIGURE 6: Internal relative moisture content of concrete under 20°C, 80% RH. (a) No CPF liner. (b) Lateral surfaces covered by CPF liner. (c) Three surfaces covered by CPF liner.

of 5 mm was lower than 80%, while the value at the depth of 20 mm was higher than 85%. The results indicated serious water loss on the surface concrete, which led to imperfect hydration, coarser pores, and higher porosity. More details about the pore distribution results are presented in Section 3.3.

CPF liner can absorb free water from plastic concrete, and then, the absorbed water could be released afterward during the drying period to improve the hydration of surface concrete. The internal relative moisture content of concrete with two surfaces or three surfaces covered by CPF liner was presented in Figures 5(b), 5(c), 6(b), and 6(c). At 20°C and 60% RH, the internal relative moisture content at the depth of 5 mm was 77%, 83%, and 85%, respectively for concrete without CPF liner, with two surfaces and three surfaces covered by CPF liner. Under the

same environment condition, the value at the depth of 20 mm was 88%, 88%, and 89%, respectively. It is clear that CPF liner could reduce water loss and improve performance of surface concrete, and the effective coverage of CPF liner was lower than 20 mm. Owing to the water storage effect of CPF liner, a higher internal relative moisture content of concrete was achieved, and it resulted in lower early-age shrinkage.

3.3. Mercury Intrusion Porosimetry (MIP). The pore size distribution of concrete without CPF liner (NTY) and with two surfaces covered by CPF liner (BMY) was measured by mercury intrusion porosimetry (MIP). Moreover, the MIP results were also employed to analyze

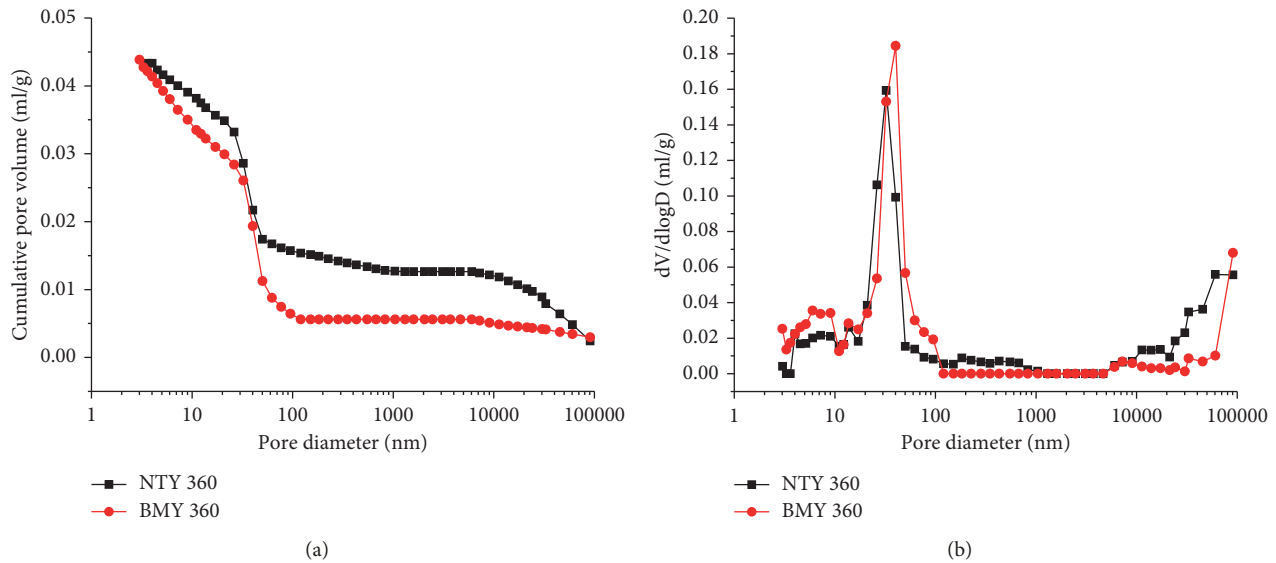


FIGURE 7: Pore distribution of concrete with and without CPF liner. (a) Integral curves. (b) Differential curves.

TABLE 2: MIP results of concrete.

Sample	Total pore volume (ml/g)	Porosity (%)	Average pore size (nm)	Pore size distribution (ml/g)			
				3~10 nm	10~100 nm	100~1000 nm	>1000 nm
NTY360	0.043	10.6	32	0.0051	0.0228	0.0027	0.0127
BMY360	0.061	9.95	40	0.0104	0.0279	0	0.0056

the porosity and the average pore size of each sample. The experimental results are presented in Figure 7 and Table 2.

Figure 7(a) presents integral curves of pore size distribution, and Figure 7(b) shows derivative of the cumulative pore volume with respect to the logarithm of the pore diameter. From Figure 7(a), it could be found that the integral curve of concrete with CPF liner was much lower than that of concrete without CPF liner, when the pore size was larger than 100 nm. However, the two curves reached similar value at the end. It means, two samples had almost the same porosity, and more coarse pores were found in the concrete without CPF liner. As presented in Table 2, the porosity of concrete without CPF liner and with two surfaces covered by CPF liner was 10.6% and 10.0%, respectively, while the average pore diameter of the two samples was 40 nm and 32 nm, respectively. According to Figure 7(b) and Table 2, there were a lot of pores with a diameter of 10~100 μm in the concrete without CPF liner, but these pores were eliminated by the application of CPF liner. In contrast, much more pores with a diameter less than 10 nm (gel pores) were formed in the concrete covered by CPF liner. Liu et al. [15] found similar results, and they concluded that the effective working zone of CPF liner was lower than 5 mm. The formation of more gel pores suggested higher hydration degree in the concrete covered with CPF liner, which was benefited from the water storage and release from CPF liner during the drying stage.

4. Conclusions

From the results obtained in the present investigation, the following conclusions are drawn:

- (1) CPF liner covered on the surface of concrete mitigated early-age shrinkage effectively. Under the temperature of 20°C and the relative humidity of 60%, two-surface-covering and three-surface-covering CPF liner decreased the shrinkage at 7 d by 44% and 48%, respectively, comparing with concrete without CPF liner covered on it.
- (2) CPF liner significantly improved the internal relative moisture content of surface concrete. At 20°C and 60% RH, the internal relative moisture content of concrete at the depth of 5 mm was 77%, 83%, and 85% respectively for concrete without CPF liner, with two surfaces and three surfaces covered by CPF liner. The higher internal relative moisture content led to further hydration degree and lower early-age shrinkage value. It should be noted that the effective depth of CPF liner was lower than 20 mm.
- (3) Covering concrete with CPF liner did not decrease the porosity of concrete significantly, but much more pores with a diameter less than 10 nm (gel pores) were formed owing to the use of CPF liner. The average pore diameter of the two samples, without and with CPF liner covering on concrete surface, was 40 nm and 32 nm, respectively.

Data Availability

The data used to support the findings of this study are included within the article.

Conflicts of Interest

The authors declare that they have no conflicts of interest.

Acknowledgments

This project was supported by the National Key R&D Program of China (No. 2017YFB0309905), National Natural Science Foundation of China (No. 51708060), Open Funds from State Key Laboratory of High Performance Civil Engineering Materials (No. 2016CEM09), and State Key Laboratory of Green Building Materials, Chongqing Commission on Housing and Urban-Rural Development (No. 2018-1-3-5,6).

References

- [1] M. H. Zhang, C. T. Tam, and M. P. Leow, "Effect of water-to-cementitious materials ratio and silica fume on the autogenous shrinkage of concrete," *Cement and Concrete Research*, vol. 33, no. 10, pp. 1687–1694, 2003.
- [2] M. Collepardi, A. Borsoi, S. Collepardi, J. J. Ogoumah Olagot, and R. Troli, "Effects of shrinkage reducing admixture in shrinkage compensating concrete under non-wet curing conditions," *Cement and Concrete Composites*, vol. 27, no. 6, pp. 704–708, 2005.
- [3] W. Sun, H. Chen, X. Luo, and H. Qian, "The effect of hybrid fibers and expansive agent on the shrinkage and permeability of high-performance concrete," *Cement and Concrete Research*, vol. 31, no. 4, pp. 595–601, 2001.
- [4] D. Cusson and T. Hoogeveen, "Internal curing of high-performance concrete with pre-soaked fine lightweight aggregate for prevention of autogenous shrinkage cracking," *Cement and Concrete Research*, vol. 38, no. 6, pp. 757–765, 2008.
- [5] C. Schröfl, V. Mechtcherine, and M. Gorges, "Relation between the molecular structure and the efficiency of super-absorbent polymers (SAP) as concrete admixture to mitigate autogenous shrinkage," *Cement and Concrete Research*, vol. 42, no. 6, pp. 865–873, 2012.
- [6] X. S. Huo and L. U. Wong, "Experimental study of early-age behavior of high performance concrete deck slabs under different curing methods," *Construction and Building Materials*, vol. 20, no. 10, pp. 1049–1056, 2006.
- [7] H. Figueiras, S. Nunes, J. S. Coutinho, and J. Figueiras, "Combined effect of two sustainable technologies: self-compacting concrete (SCC) and controlled permeability formwork (CPF)," *Construction and Building Materials*, vol. 23, no. 7, pp. 2518–2526, 2009.
- [8] D. W. Law, T. Molyneaux, and T. Aly, "Long-term performance of controlled permeability formwork," *Australian Journal of Civil Engineering*, vol. 15, no. 2, pp. 117–125, 2017.
- [9] Z. Tian and P. Qiao, "Multiscale performance characterization of concrete formed by controlled permeability formwork liner," *Journal of Aerospace Engineering*, vol. 26, no. 4, pp. 684–697, 2013.
- [10] S. Kothandaraman and S. Kandasamy, "The effect of controlled permeable formwork (CPF) liner on the surface quality of concretes," *Cement and Concrete Composites*, vol. 76, pp. 48–56, 2017.
- [11] S. Kothandaraman and S. Kandasamy, "The effect of controlled permeable formwork liner on the mechanical properties of concrete," *Materials and Structures*, vol. 49, no. 11, pp. 4737–4747, 2016.
- [12] S. Kothandaraman, S. Kandasamy, and K. Sivaraman, "The effect of controlled permeable formwork liner on the mechanical and durability properties of self compacting concrete," *Construction and Building Materials*, vol. 118, pp. 319–326, 2016.
- [13] A. A. Adam, D. W. Law, T. Molyneaux, I. Patnaikuni, and T. Aly, "The effect of using controlled permeability formwork on the durability of concrete containing OPC and PFA," *Australian Journal of Civil Engineering*, vol. 6, no. 1, pp. 1–12, 2010.
- [14] D. W. Law, T. Molyneaux, I. Patnaikuni, and A. A. Adam, "The site exposure of concrete cast using controlled permeability formwork," *Australian Journal of Civil Engineering*, vol. 10, no. 2, pp. 163–176, 2012.
- [15] J. Liu, C. Miao, C. Chen, J. Liu, and G. Cui, "Effect and mechanism of controlled permeable formwork on concrete water adsorption," *Construction and Building Materials*, vol. 39, pp. 129–133, 2013.
- [16] K. Yang, M. Zhong, B. Magee et al., "Investigation of effects of Portland cement fineness and alkali content on concrete plastic shrinkage cracking," *Construction and Building Materials*, vol. 144, pp. 279–290, 2017.
- [17] K. Ichise, K. Nagao, and S. Nakane, "Method of measuring moisture content in content heated to high temperature," Report, vol. 32, pp. 107–111, Obayashi Corporation Technical Research Institute, Kiyose, Japan, 1986.
- [18] T. M. Chrisp, W. J. McCarter, G. Starrs, P. A. M. Basheer, and J. Blewett, "Depth-related variation in conductivity to study cover-zone concrete during wetting and drying," *Cement and Concrete Composites*, vol. 24, no. 5, pp. 415–426, 2002.
- [19] D.-W. Ryu, J.-W. Ko, and T. Noguchi, "Effects of simulated environmental conditions on the internal relative humidity and relative moisture content distribution of exposed concrete," *Cement and Concrete Composites*, vol. 33, no. 1, pp. 142–153, 2011.
- [20] B. Kucharczyková, L. Topolář, P. Daněk, D. Kocáb, and P. Misák, "Comprehensive testing techniques for the measurement of shrinkage and structural changes of fine-grained cement-based composites during ageing," *Advances in Materials Science and Engineering*, vol. 2017, Article ID 3832072, 10 pages, 2017.
- [21] A. Leemann, P. Nygaard, and P. Lura, "Impact of admixtures on the plastic shrinkage cracking of self-compacting concrete," *Cement and Concrete Composites*, vol. 46, pp. 1–7, 2014.
- [22] T. A. Hammer, "Effect of silica fume on the plastic shrinkage and pore water pressure of high-strength concretes," *Materials and Structures*, vol. 239, no. 5, pp. 273–278, 2001.
- [23] J. Zhang, H. Dongwei, and S. Wei, "Experimental study on the relationship between shrinkage and interior humidity of concrete at early age," *Magazine of Concrete Research*, vol. 62, no. 3, pp. 191–199, 2010.



Hindawi
Submit your manuscripts at
www.hindawi.com

